Corey, A.T. 1994. Mechanics of immiscible fluids in porous media. Water Resources Publications, Highlands Ranch, CO.
Duley, F.L. 1939. Surface factors affecting the rate of intake of water by soils. Soil Sci. Soc. Am. Proc. 4:60–64.
Eigel, J.D., and I.D. Moore. 1983. Effect of rainfall energy on infiltration into a bare soil. p. 188–199. *In* Advances in infiltration. Proc. Natl. Conf. Advances in Infiltration, Chicago, IL. 12–13 Dec. 1983. ASAE, St. Joseph, MI.
Ellison, W.D., and C.S. Slater. 1945. Factors that affect surface sealing and infiltration of exposed soil surface. Agric. Eng. 26:156–157.
Lang, P.M., and J.B. Mallett. 1984. Effect of the amount of surface maize residue on infiltration and soil loss from a clay loam soil. S. Afr. J. Plant Soil 1:97–98.
McIntyre, D.S. 1958. Permeability measurements of soil surface seals formed by raindrop impact. Soil Sci. 85:185–189.
Morin, J., and Y. Benyamini. 1977. Rainfall infiltration into bare soils. Water Resour. Res. 13:813–817.
Mualem, Y., and S. Assouline. 1989. Modeling soil seal as a nonuniform layer. Water Resour. Res. 25:2101–2108.
Mualem, Y., S. Assouline, and D. Eltahan. 1993. Effect of rainfall-induced soil seals on soil water regime: Wetting processes. Water Resour. Res. 29:1651–1659.
Philip, J.R. 1998. Infiltration into surface-sealed soils. Water Resour. Res. 34:1919–1927.
Rawls, W.J., D.L. Brukensiek, J.R. Simanton, and K.D. Kohl. 1990. Development of a surface-seal factor for a Green Ampt model. Trans. ASAE 33:1224–1228.
RZWQM Development Team: J.D. Hanson, L.R. Ahuja, M.D. Shaffer, K.W. Rojas, D.G. DeCoursey, H. Farahani, and K. Johnson. 1998. RZWQM: Simulating the effects of management on water quality and crop production. Agric. Syst. 57:161–195.
Savabi, M.R., and D.E. Stott. 1994. Plant residue impact on rainfall interception. Trans. ASAE. 37:1093–1098.
Simunek, J., T. Vogel, and M.Th. van Genuchten. 1994. The SWMS–2D code for simulating water flow and solute transport in two-dimensional variably saturated media. Version 1.2, Res. Rep. 132. U.S. Salinity Laboratory, USDA-ARS, Riverside, CA.
Smith, R.E., C. Corradini, and F. Melone. 1999. A conceptual model for infiltration and redistribution in surface-sealed soils. Water Resour. Res. 35:1385–1393.
Tackett, J.L., and R.W. Pearson. 1965. Some characteristics of soil surface seals formed by simulated rainfall. Soil Sci. 99:407–412.
Unger, P.W., and B.A. Stewart. 1983. Soil management for efficient water use: An overview. p. 419–460. *In* H.M. Taylor et al. (ed.) Limitations to efficient water use in crop production. ASA, CSSA, and SSSA, Madison, WI.
Van Genuchten, M.Th. 1980. A closed-form equation for predicting the hydraulic conductivity of unsaturated soils. Soil Sci. Soc. Am. J. 44:892–898.

Effect of Sediment Load on Soil Detachment and Deposition in Rills

G. H. Merten, M. A. Nearing,* and A. L. O. Borges

ABSTRACT

According to theory, the rate of detachment of soil particles in rills is reduced as a first-order function of the amount of sediment load in the flow. The first objective of this study was to determine if experimental results confirmed current detachment-transport coupling theory. The second objective was to investigate two hypothesized mechanisms responsible for any coupling effect observed: The first mechanism was that since turbulence is known to be a critical factor in detachment by flow, and since it is also known that sediment in water reduces turbulent intensity, it was suggested that sediment in flow reduces detachment via a correspondent reduction in turbulent intensities. This hypothesis was tested indirectly by adding a sediment load that was carried entirely in the suspended state. The second mechanism was that sediment covering the soil bed during the erosion process shields the soil from the forces of flow, thus reducing detachment. This hypothesis was tested by introducing bed-load sediment. Sediment loads exiting the rill and detachment and deposition along the rill were measured. Detachment was reduced and deposition increased as a linear function of the amount of sediment introduced into the flow. Results indicated that, in general, detachment did decrease according to current theory, but discrepancies in the erosional patterns were observed, which none of the current models explain. Both hypothesized mechanisms of reduction in detachment rates were apparently active in reducing detachment rates, though the shielding mechanism appeared to have a greater impact than did the mechanism associated with a reduction in turbulent intensity.

Concentrated surface water flow is capable of detaching and transporting sediments from the soil mass. The energy for these processes is provided, basically, by the weight of the mixture of water and sediment and the downslope gradient of the flow. Studies related to the mechanics of rill erosion have shown that rates of soil detachment are inversely dependent upon the magnitude of the sediment load at a given time and location on the soil surface (Meyer and Monke, 1965; Rice and Wilson, 1990; and Cochrane and Flanagan, 1996). The theoretical basis for this effect has been discussed by Foster and Meyer (1972) and Hairsine and Rose (1992a, 1992b).

Foster and Meyer (1972) (later presented in more detail by Foster, 1982) support the hypothesis that the flow possesses finite energy, which may be expended either to detach soil particles from the bulk soil mass or to transport previously detached sediments. Within this framework, it might be considered that the energy required to sustain movement of the sediment in transit, as well as to initiate movement of previously detached sediment particles resting on the bottom of the bed, is less than the energy necessary to detach new sediments from the soil mass. In this way, the energy is preferentially used for those processes related to the continuation of movement of the sediments. Any excess energy could then be available for detachment.

In the conceptual model of Foster and Meyer (1972), the flow energy available for detachment is calculated as the difference between sediment transport capacity minus the energy used for transport, represented by the sediment load in transit. Thus to estimate the rates of detachment it is essential to determine transport capacity.

A second theoretical model for the utilization of flow energy is that of Hairsine and Rose (1992a, 1992b). In this model, Hairsine and Rose propose that flow energy,

G.H. Merten and A.L.O. Borges, Hydraulic Research Institute, Federal Univ. of Rio Grande do Sul, Box 15029, CEP 91501, Porto Alegre - RS, Brazil; M.A. Nearing, USDA-ARS National Soil Erosion Research Lab., Soil Bldg., Purdue Univ., West Lafayette, IN 47907-1196. Received 18 Jan. 2000. *Corresponding author (mnearing@purdue.edu).

Published in Soil Sci. Soc. Am. J. 65:861–868 (2001).

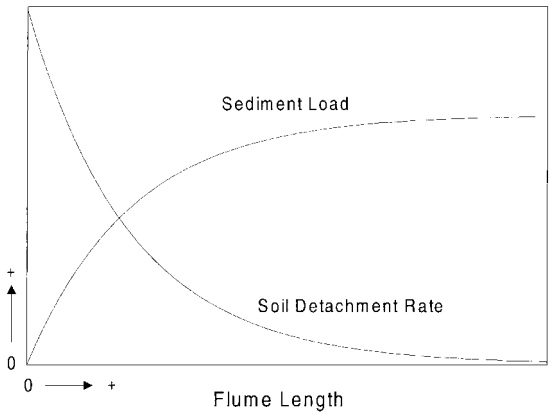

Fig. 1. Schematic diagram of theoretical results for the case of a first-order relationship between sediment load and local detachment rate in a rill. This example is for the case of uniform bed slope, constant and uniform flow rate, and no introduction of sediment from the upper end or sides of the rills.

represented by the stream power of the flow (Ω), is used by four processes (i) to overcome the threshold of entrainment of the cohesive medium to initiate the process of detachment, (ii) entrainment (detachment) of soil from the bed, (iii) entrainment of previously detached sediments that are found on the bottom of the stream bed, and (iv) dissipation of energy as heat and noise. Hairsine and Rose's model also puts forth the proposition that continuous deposition causes sediments to be deposited over the stream bed, which creates a layer that protects the bottom of the bed from erosive forces.

Both models for soil erosion by flow (Foster and Meyer, 1972; Hairsine and Rose, 1992b) produce results that are somewhat similar in terms of soil detachment and sediment load as a function of downslope distance in a rill. Both are essentially first-order models. Given the simple case of constant slope and discharge with downslope distance, the models will predict an exponentially decaying rate of detachment with distance as sediment load increases. Sediment load will approach an equilibrium concentration representing a transport limiting state (Fig. 1). In the case of the Foster and Meyer model, this state is interpreted as the condition when all available flow energy is being used to transport sediment and no energy remains to detach new sediment particles from the soil mass. In the case of the Hairsine and Rose scenario, the soil bed has reached a state of high sediment cover and is well-protected, and the instantaneous rate of sediment deposition equals the instantaneous rate of sediment entrainment. Both the Foster and Meyer model (1972) and the Hairsine and Rose model (1992a, 1992b) have been incorporated in modified forms into practical, field-scale models of erosion (Foster et al., 1981; Nearing et al., 1989; and Rose et al., 1998).

Lei et al. (1998) developed a more sophisticated, finite-element model for rill erosion that took into account the morphological development of the rill during the erosion process, especially the circular feedback loop between flow hydraulics, which drives the erosion process, erosion which causes morphological changes in the rill slope and width, and the impact of the changing bed morphology on hydraulics of flow (Nearing et al., 1997). The results of this model were tested using the same soil (in a different experimental setup) as is used in the current study. The results of Lei et al.'s (1998) model indicated that the erosion process in the rill can be somewhat more complex than described by the earlier models.

Turbulence is a critical component of soil erosion in rills. While typical soil tensile strength are of the order of kilopascals, even for unconsolidated soils (Nearing et al., 1991), typical average shear stresses of flow are only of the order of pascals. Soil detachment occurs only because localized events of high-intensity turbulence known as "bursting" produce large fluctuations in stresses on the more weakly bound areas at the soil surface with enough energy to dislodge sediment from the soil mass (Nearing, 1991). It has been empirically shown that without turbulence, detachment of soil by flow does not occur (Nearing and Parker, 1994). The presence of a high concentration of sediment in runoff has a considerable effect on the velocity profile and turbulence structure. The presence of fine sediment, which is primarily moved in suspension, reduces the intensity of the turbulence (Einstein and Ning Chien, 1955; Vanoni and Namicos, 1960; Wang and Larson, 1994). Given this, it would be reasonable to hypothesize that a reason for reduction in the rate of detachment with increased sediment load may be due to a reduction in turbulent intensities imparted to the soil bed when sediment is in the flow.

The objectives of this study were twofold. The first objective was to measure the effect of increasing sediment load in the flow of a confined rill on the spatial, downslope distribution of detachment and deposition under conditions of constant flow rate of water and constant slope. This enabled us to evaluate the utility of the first-order relationships suggested in the models of Foster and Meyer (1972) and of Hairsine and Rose (1992a, 1992b). The second objective was to investigate the mechanism responsible for the process whereby soil detachment rate decreases when sediment load is present. This was done by introducing bed load–size sediment in one case and suspended load–size sediment in the second case, and again investigating the spatial, downslope distribution of detachment and deposition under conditions of constant flow rate of water and constant slope.

MATERIALS AND METHODS

A series of aluminum boxes were mounted on a variable-slope flume. The dimensions were as follows: four boxes of 0.10 by 0.10 by 0.25 m; six boxes of 0.10 by 0.10 by 0.50 m; and four boxes of 0.10 by 0.10 by 1.00 m. The boxes were connected to form a small, rectangular canal 8 m long. Known quantities of dry, sieved (2.5 mm) soil were placed in the boxes. The soil used in the experiments was a Cecil sandy loam (fine, kaolinitic, thermic Typic Kanhapludults) from Georgia, containing 714 g kg^{-1} of sand, 174 g kg^{-1} of silt, 113 g kg^{-1} of clay. Dry aggregate size of the material after screening was distributed according to D_5 = 140 μm, D_{10} = 170 μm, D_{50} = 650 μm, and D_{90} = 1830 μm.

Table 1. Sediment input rates, flow rates, and times for the experiments.

Exp.	Input material	Repetition	flow rate	Total time	Steady time
			$m^3 s^{-1}$	s	
1	Clear water	1	0.000084	245.2	206.0
		2	0.000083	187.6	150.5
		3	0.000091	233.4	191.0
	Soil	1	0.000090	233.3	200.0
	2.03 g s^{-1}	2	0.000090	230.6	200.0
		3	0.000089	229.0	190.0
	Soil	1	0.000085	230.7	206.0
	3.81 g s^{-1}	2	0.000088	226.0	195.0
		3	0.000089	230.7	195.0
	Soil	1	0.000074	244.3	197.6
	6.13 g s^{-1}	2	0.000087	232.4	184.7
		3	0.000084	227.1	181.0
	Soil	1	0.000073	242.9	198.7
	7.49 g s^{-1}	2	0.000083	249.4	198.8
		3	0.000084	233.7	186.1
2	Fine beads	1	0.000065	228.5	183.5
	0.9 g s^{-1}	2	0.000075	232.7	185.7
		3	0.000083	243.5	194.1
	Coarse beads	1	0.000069	248.1	200.5
	0.8 g s^{-1}	2	0.000063	237	189.7
		3	0.000082	233.2	185.7
	Fine beads	1	0.000071	239.3	199.3
	3.3 g s^{-1}	2	0.000062	237.6	203.5
		3	0.000069	235	192.5
	Coarse beads	1	0.000054	234.3	195.4
	3.1 g s^{-1}	2	0.000052	242.7	190
		3	0.000075	242.2	197.8

A sediment feeder was mounted to the upper end of the canal to inject a specified amount of sediment into the flow before the runoff reached the soil in the boxes. The material used as sediment in the first experiment was the same soil (Cecil) used as the bed material, while the second experiment used two sizes of uniform glass beads equivalent to coarse silt (39 μm) and coarse sand (510 μm).

The treatments for the two experiments are listed in Table 1. The experimental plan within each of the two experiments was conducted in random order and each treatment was replicated three times.

After connecting the boxes, which together formed a usable rectangular length below the sediment input feeder of 7.6 m long, dry soil was placed in each box in quantities corresponding to the box size: 1166 g in the 0.25-m-long boxes, 2333 g in the 0.50-m-long boxes, and 4666 g in the 1.00-m-long boxes. The surface of the soil was leveled and lightly packed, forming a layer of soil 4 cm deep, with a bulk density of approximately 1.17 Mg m^{-3}. After preparing the boxes, the flume that contained the boxes was leveled and then filled with water until the water level was even with the soil surface in the boxes. The bottoms of the boxes were perforated to allow the free flow of water into the boxes during satiation and free drainage when the experiment was run. The time allowed for satiation in all the trials was 1 d.

Thirty minutes before beginning the trial, the water in the canal was drained and the slope was adjusted. Bed slope was set to 5%. Target inflow rate of water was 0.122 L s^{-1}. Water temperature was 20°C ± 1°C in every experimental run except for Replication 1 for the coarse beads treatment of 0.8 g s^{-1}, when the water temperature was measured at 18°C. After calibrating the flow rate and solid-load input rate, the trial was begun with the simultaneous addition of water and sediment. During the trial, samples of flow were collected continuously in bottles at the end of the canal. The velocity of the runoff was determined at the same time as the samples were collected using fluorescent dye over a distance of 4 m in the canal between the points of 0.60 and 4.60 m. The velocity values were corrected based on an equation suggested by Li et al. (1996), who, due to the difficulty in determining the centroid of tracer plumes, proposed a correction factor for leading edge velocity defined by the following equation:

$$\alpha = 0.251 - 0.327 \log S + 0.114 \log \mathrm{Re} \qquad [1]$$

where S (m m^{-1}) is the slope and Re is the Reynolds number.

Once the trial had run, the supply of water and sediment was stopped. This interval of time was considered the period of steady flow (Table 1), while the total time for the trial is measured until the moment there is no more flow from the end of the canal. To determine the concentration of sediments in the flow, the bottles of flow collected during the experiment were later weighed, alum was added to induce flocculation, and the bottles were left to settle overnight. The following day, the water in the jars was poured off and the remainder was dried in an oven at 105°C for approximately 48 h. The sediment load was calculated as the product of the flow rate and the concentration of sediments.

After the run, the boxes of the canal were separated and placed in an oven to dry at 60°C for about 4 d, until their weight remained constant. To determine the correct time to remove the boxes from the oven, an additional box of 0.1 by 0.1 by 1.0 m was prepared in the same way as the others and then set aside. After the trial was run, this additional box was placed with the others in the oven and allowed to dry until it reached the same weight it had before inundation, at which point all the boxes were removed. The boxes were then weighed so that the rates of detachment and deposition along the length of the canal could be determined by subtracting the difference in weight from before and after the trial was run and considering the total time of the trial.

A portion of the sediment eroded from the flume was not collected in jars, but was deposited in a bucket. This material was used to determine particle size of the sediment. The sediment was sorted using the following process: using a gentle flow of water, the wet sediment that was collected in the bucket after the trial had run its course was passed through

Table 2. Sediment load and concentration, detachment, and deposition results for the experiments.

Exp.	Input material	Rep	Sediment load	Sediment concentration	Total detachment	Total deposition	Length to deposition
			g s^{-1}	g L^{-1}	g		m
Control	Clear water	1	5.12	60.72	1541.7	366	0.206
		2	6.02	72.25	1465.4	438.6	0.266
		3	6.02	65.72	1480.2	376.2	0.1822
		Avg.	5.72	66.23	1495.8	393.6	0.218
1	Soil	1	5.99	66.63	1221.9	520.4	0.270
	2.04 g s^{-1}	2	6.11	68.09	1256.2	235.8	0.210
		3	6.01	67.20	1265.5	480.3	0.198
		Avg.	6.04	67.31	1247.9	412.2	0.226
	Soil	1	6.23	73.34	934.6	520.6	0.190
	3.81 g s^{-1}	2	6.57	74.70	790.7	651.8	0.186
		3	6.52	73.46	854.3	627.9	0.162
		Avg.	6.44	73.83	859.9	600.1	0.179
	Soil	1	5.85	79.41	577	645.2	0.182
	6.13 g s^{-1}	2	6.93	79.95	764.8	678	0.186
		3	6.52	77.22	453.8	664.1	0.178
		Avg.	6.43	78.86	598.5	662.4	0.182
	Soil	1	4.99	69.20	277.6	1019.6	0.122
	7.49 g s^{-1}	2	7.22	86.73	324.4	792.4	0.150
		3	6.12	73.12	237.4	1022.9	0.054
		Avg.	6.11	76.35	279.8	945.0	0.109
2	Fine beads	1	5.13	71.27	1167.1	703.1	0.210
	0.9 g s^{-1}	2	7.09	86.26	1222.7	579.8	0.170
		3	6.74	75.39	1541.4	565.9	0.170
		Avg.	6.32	77.64	1310.4	616.3	0.183
	Coarse beads	1	6.01	81.48	1306.8	609.7	0.170
	0.8 g s^{-1}	2	5.52	80.91	1171.5	774.3	0.170
		3	7.19	83.11	1422.7	560.8	0.170
		Avg.	6.24	81.83	1300.3	648.3	0.170
	Fine beads	1	6.22	86.98	1503.5	1022	0.290
	3.3 g s^{-1}	2	4.87	74.32	1030.4	689.8	0.350
		3	5.26	71.40	1020.2	386.3	0.410
		Avg.	5.45	77.57	1184.7	699.4	0.350
	Coarse beads	1	3.39	61.95	739.5	630.2	0.210
	3.1 g s^{-1}	2	3.58	62.12	633.8	788.2	0.190
		3	5.37	65.31	709.8	482.1	0.170
		Avg.	4.11	63.13	694.4	633.5	0.190

a series of sieves with mesh sizes of 2000, 1000, 500, 250, 210, 105, and 53 μm. The different fractions collected were then placed in the oven to dry at 60°C until they attained a constant weight.

RESULTS AND DISCUSSION

Outflow rates and time of both Exp. 1 and 2 are reported in Table 1. The velocity of flow was not statistically different ($\alpha = 0.05$) between any of the treatments. Average measured flow velocity was 0.22 m s^{-1}. Erosion results are reported in Table 2, and the results of the sieve analyses on the sediment are reported in Table 3.

Experiment 1: Soil Used as Sediment Input Material

In each experimental test, a portion of the rill bed experienced net detachment and a portion experienced net deposition (Fig. 2). A portion of the deposition along the rill may have been due to deposition of the sediment in the flow during the receding limb of the runoff curve, between the time the water source was turned off and the time the water stopped flowing off the soil bed. If we use the runoff rates for water and sediment and the time of the recession limb, and if we assume that 100% of the sediment that was in the flow when the water was turned off deposited before reaching the end, we obtain an upper-bound estimate for the amount of the deposition that might be attributed to the recession limb effect. Using average values for runoff rates and times, this upper bound was calculated to be 235 g. Clearly, the receding limb effect cannot explain the majority of the deposition observed in these experiments (Table 2). The result of net deposition observed on portions of the initially uniform-sloped soil beds for each test is

Table 3. Weight percentage of the different class sizes of the transported sediment for Exp. 1.

Sieving class	Weight percentage				
	0 g s^{-1}†	2.03 g s^{-1}	3.81 g s^{-1}	6.13 g s^{-1}	7.49 g s^{-1}
mm	%				
2	10.3	11.1	11.7	10.2	9.6
2–1	31.8	32.6	27.3	29.1	29
1–0.5	19.6	24.1	22.1	22.8	20
0.5–0.25	14.5	10.3	13.6	14.7	14.9
0.25–0.21	7.4	3.6	3.6	4.8	5.4
0.21–0.105	5.5	6.4	7.1	6.2	7.2
0.105–0.053	3.4	3.4	4.4	4.6	4.5
0.053–0.003	7.5	8.5	10.3	7.6	9.4

† Rate of sediment injected.

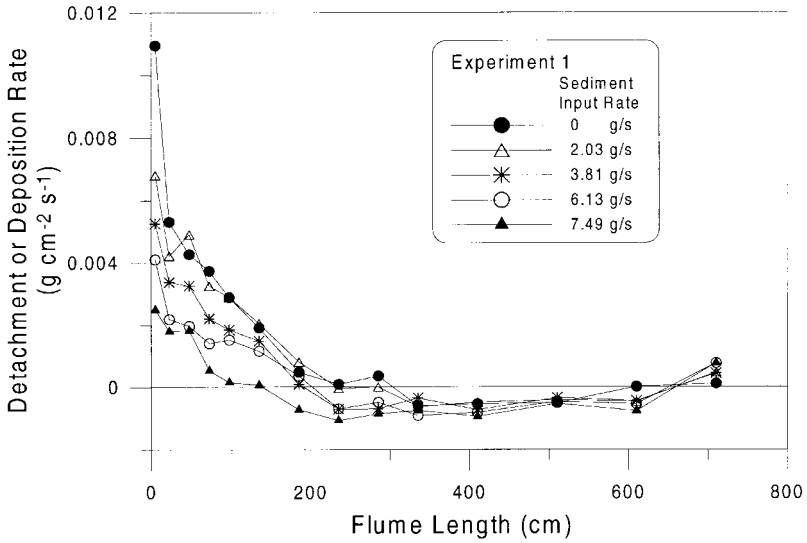

Fig. 2. Measured average rate of soil detachment and sediment deposition along the rill length for Exp. 1 based on the weight of the soil in the boxes before and after the experimental tests. Sediment input was from the upper end of the flume.

consistent with neither the Foster and Meyer (1972) model nor the Hairsine and Rose (1992a, 1992b) model. For the case of constant slope and no lateral inflow of sediment along the rill (either from interrill erosion or sidewall sloughing), these models would predict net detachment with a gradual approach to zero detachment rate along the length of the rill. The same holds true for the model of Lei et al. (1998) for the application of the appropriate case, which is "time invariant and spatially uniform flow widths and time variant and spatially non-uniform slopes." In the model of Lei et al. (1998), deposition along an initially uniform bed slope did occur for the case where the rill in the model computations was allowed to widen and narrow in response to the processes of detachment and deposition, but not for the case in the model runs where width of flow was held constant. Rill widening induces a shallower flow and a correspondent reduction in flow transport capacity, which can trigger a mode of net deposition, shallower and wider flow, etc. The metal sidewalls of the canal used in the current experiment, however, prevented changes in the rill width.

Incremental increases in sediment inflow for Exp. 1 using the soil material as inflow sediment caused incremental changes in the pattern of erosion in the rill as expected (Fig. 2). For the case of clear water and the two lower sediment input rates, total detachment exceeded total deposition in the rill; for the two higher sediment input rates, total deposition exceeded total detachment in the rill (Table 2). It is interesting that even for the two cases where sediment input levels exceeded the transporting capacity of the flow, that is, for the sediment input rates of 6.13 and 7.49 g s^{-1}, net detachment was observed in the upper end of the flume. This result is in a sense complementary to the observation that all treatments experienced areas of net deposition in the flume: all treatments also experienced areas of net detachment, even in the case where deposition was predominant overall.

This phenomenon is seen more clearly in the graph of average sediment load as a function of downslope distance (Fig. 3). It appears that there is some type of "overshooting" in terms of sediment load that took place. In other words, the sediment load increased to a certain point and then began to decline again to its final value at the end of the flume. Obviously, we do not have information on what the pattern might look like if it were to be continued further in distance. In the experiments reported by Lei et al. (1998), an oscillatory pattern of alternating detachment and deposition was observed in the flume, but in that case the result was attributed to the alternating widening and narrowing of the rill width. This interpretation was supported by the results of the simulation studies. The observation of the "overshoot" phenomenon in the rill sediment load was also reported from field studies by Huang et al. (1996) when the sediment regime shifted from a detachment to a transport-limiting situation. However, in the current experimental results reported here, the rill was not allowed to vary in width because of the fixed borders on the channel, yet we still observed the same overshoot phenomenon. Thus the variation in flow hydraulics caused by changes in rill width and associated changes in flow depth and bed stresses are apparently not the sole reason for this overshoot phenomenon. The overshoot phenomenon may be, and probably must be, related to the flow hydraulics, but width variations are not the sole cause.

Results shown in Fig. 2 and 3 are generally consistent in form with the first-order models suggested by Foster and Meyer (1972) and by Hairsine and Rose (1992a, 1992b). In the initial length of the flume, detachment rate decays exponentially from an initial value that depends on the input rate of sediment (Fig. 2). Calculated sediment load initially increases in a manner suggested by Fig. 1 for the first-order model (Fig. 3). However, it is also clear from an examination of the measured data compared to the theoretical curves that the current models cannot explain the true patterns of observed detachment and deposition along the rill bed. The current data

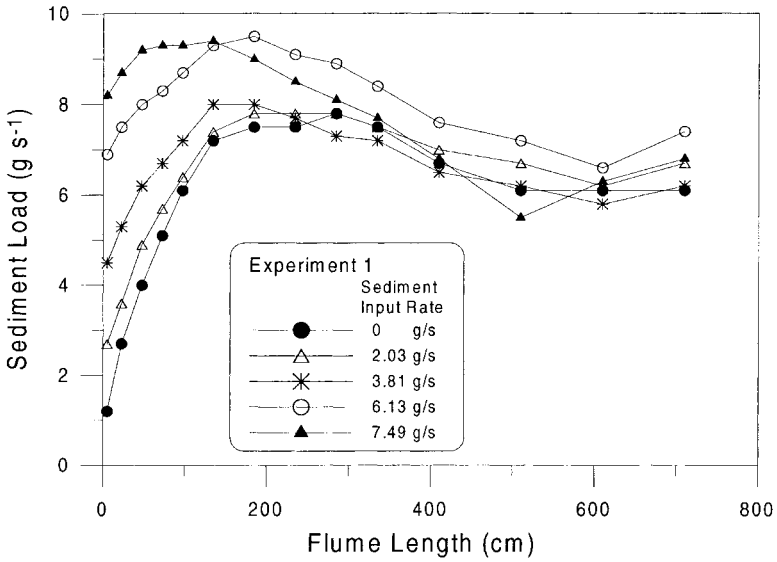

Fig. 3. Calculated average sediment load along the rill length during the experiments based on the data from Fig. 2.

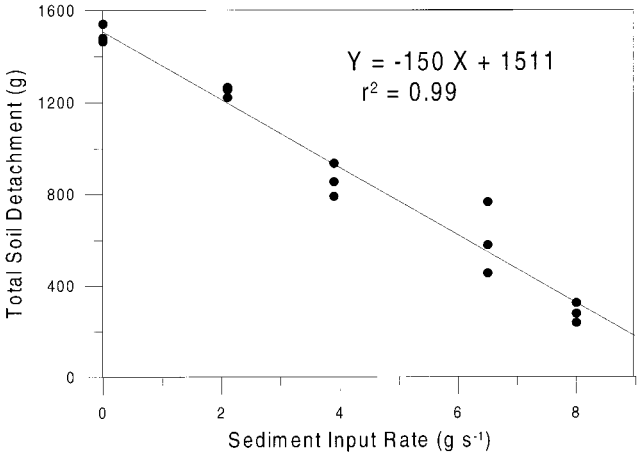

Fig. 4. Total soil detachment in the rill, based on the weight of the soil in the boxes before and after the experimental tests.

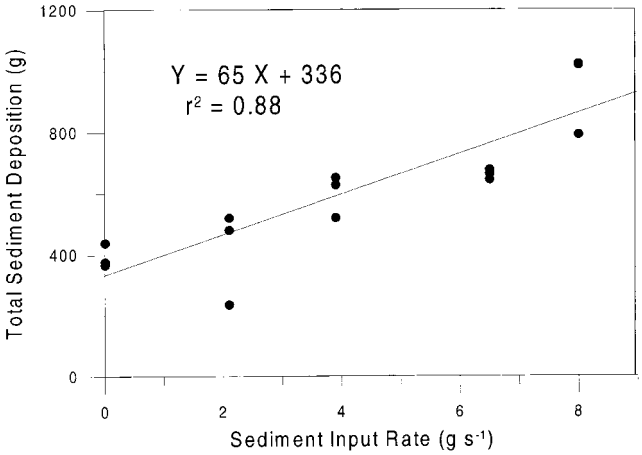

Fig. 5. Total sediment deposition in the rill, based on the weight of the soil in the boxes before and after the experimental tests.

would suggest that an element may be missing in our current mathematical descriptions of the erosion process that prevents a totally accurate estimation of the downslope distribution of erosion along the hillslope.

Overall, there was no trend for sediment load or sediment concentration as a function of sediment input rates for Exp. 1. The regression lines for those two cases were not significantly different from zero. The total soil detachment amount and the total sediment deposition amounts were both linear functions of the sediment input rates, with measured detachment decreasing (Fig. 4) and measured deposition increasing (Fig. 5) as the input load increased.

Experiment 2: Uniform Glass Beads Used as Sediment Input Material

In general terms, the results for Exp. 2 where uniform glass beads were used as sediment input material were similar to the results for Exp. 1. All treatments resulted in areas on the rill of both net detachment and net deposition, and the total detachment was reduced and total deposition was increased relative to the treatment of clear water (Table 2). For the lower input rates of sediment, the coarse and fine beads acted similarly (Table 2; Fig. 6a). However, for the higher level of sediment input rates, the coarse beads treatment did have significantly less ($\alpha = 0.05$) total detachment than did the fine beads treatment. This occurred despite the fact that the inflow rate of coarse beads was slightly less (3.1 g s^{-1}) than for the fine beads (3.3 g s^{-1}). The pattern of detachment was also different for the coarse vs. the fine beads at the higher input rate (Fig. 6b). While the detachment rate was lower in the upper end of the flume for the case of the fine beads compared with the coarse beads, the detachment rate remained relatively constant for approximately 2 m before it began to decline in the case of the fine beads.

Bed-Load and Suspended-Load Classifications

To determine the mode of transport of the sediment collected at the end of the canal, a relation proposed by Raudkivi (1990) was used. The mode of transport was estimated by the relationship between velocity of sedimentation (w) (m s^{-1}) and the shear velocity on

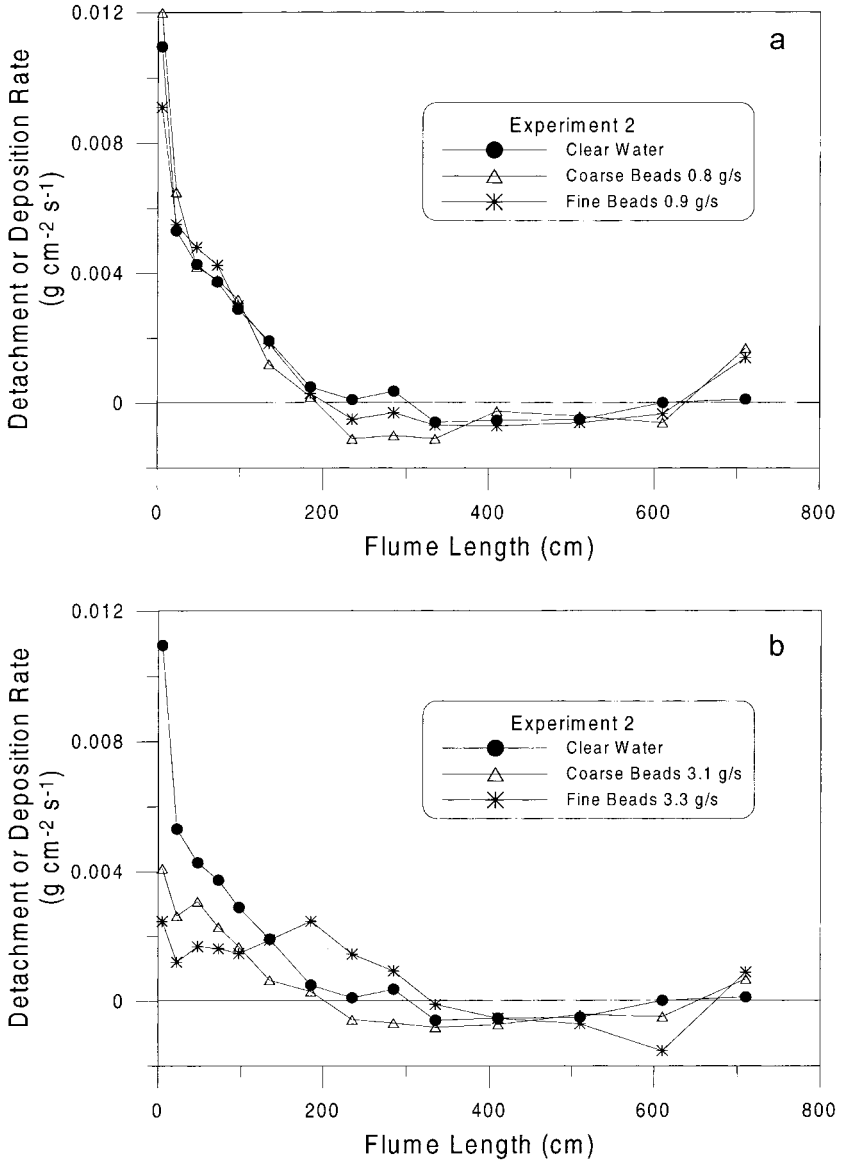

Fig. 6. Measured average rate of soil detachment and sediment deposition along the rill length for Exp. 2, based on the weight of the soil in the boxes before and after the experimental tests: (a) for the lower rates of sediment input, and (b) for the higher rates of sediment input. Sediment input was from the upper end of the flume.

the bottom (u_*) ($gR_hs^{1/2}$), according to the following criteria: sediment within the range $2 < w/u_* < 6$ was considered to be bed load, sediment within the range $0.6 < w/u_* < 2$ was considered to be saltating load, and sediment within the range $w/u_* < 0.6$ was considered to be suspended load.

Table 4 shows the mode of transport calculated according the Raudkivi's criteria (1990) for the different rates of input of sediment for Exp. 1. The predominant mode of transport was bed load (~60%), followed by suspension (~20%) and saltation (~20%). These calculated values agree with the visual observations during the experimental runs that showed that the greater part of the sediment was transported by bed load.

For Exp. 2, the small beads had a computed value of u_*/w of 0.07, which puts it clearly into the range of suspended sediment. The coarse beads had a value of u_*/w of 2.88, which put it in the bed-load range. As sediment was picked up along the bed in both of these cases, the sediment mixture undoubtedly became more mixed in size and transport mode. For the case in Exp. 2 for the lower input sediment rates (0.8 and 0.9 g s^{-1}), the effect of the input sediment was apparently quickly superceded by the effect of the sediment detached from the bed. In this case, the behavior of the system was not noticeably different between the case of the fine vs. the

Table 4. Mode of sediment transport for Exp. 1.

Sediment input rate	Sediment transport mode		
	Bed load	Saltation	Suspension
g s^{-1}	%		
0	61.7	21.9	16.4
2.03	67.8	13.9	18.3
3.81	61.0	17.2	21.8
6.13	62.1	19.5	18.4
7.49	58.6	20.3	21.1

coarse beads, as discussed previously. For the higher input sediment rates (3.1 and 3.3 g s^{-1}), the effect of the input sediment was more predominant, evidenced by the differences in the erosional patterns for the two bead types.

A reasonable interpretation of the behavior differences between the two bead types is related to the sediment transport mode. The suspended load treatment (fine beads) significantly reduced the erosion rates relative to clear water inflow (Table 2; Fig. 6b), which supports the hypothesis that a reduction in turbulence associated with the suspended load does reduce detachment rates. The bed-load treatment (coarse beads) also reduced erosion rates relative to clear water inflow, which supports the hypothesis that protection of the soil bed associated with the bed load does reduce detachment rates. The bed load had a greater impact on the overall soil detachment than did the suspended load. Since in Exp. 1 the principal sediment load was in the form of bed load (Table 4), it is not surprising that the bed-load case in Exp. 2 (Fig. 6b, coarse sediment) followed the erosional patterns of Exp. 1 (Fig. 2) more closely than did the suspended-load case of Exp. 2 (Fig. 6b, fine sediment).

SUMMARY

The results of this study help us to understand certain processes of rill erosion, but they also bring out further questions that need to be addressed for a complete understanding. It appears clear from the experimental evidence that a significant sediment coupling relationship for rill detachment exists. Detachment rate does appear to decrease as sediment load increases, and the process appears to be consistent with a first-order process (i.e., detachment rate appears to be proportional to sediment load). It also appears clear, based on the results of the second experiment reported here, that both suspended load and bed load influence the detachment rate. We interpret this to mean that bed load protects the soil surface and thus reduces the hydraulic forces of flow that act to dislodge soil particles, and that suspended load reduces turbulent intensities that decrease instantaneous shear forces acting on the bed.

What is not entirely clear from the results is why we observed depositional zones on the uniform rill bed under constant flow conditions. We can speculate on several possible explanations for this. One possibility is that as the upper portion of the rill bed was eroded, the slope of the bed changed. This could have caused deposition to occur on the lower portion of the flume from the upstream eroded sediment. Perhaps a nonlinear reduction in turbulent bursting occurred with increased sediment load, which triggered a reduction in the sediment transport capacity in the lower sections of the flume. More research will be required to clarify this observation.

ACKNOWLEDGMENTS

This work was made possible by a research grant provided by the Brazilian government via CAPES; Purdue University; the logistical support necessary to execute the experiments from the National Soil Erosion Research Laboratory, Agricultural Research Service, United States Department of Agriculture; the interest of its general director Dr. Darrell Norton; the *prestimosa* and dedicated orientation and support of Dr. Ana Luíza de Oliveira Borges; and the indispensable help with the laboratory work offered by friends Antônio Carlos de Azevedo, Euzébio Ventura, X. C. Zhang, and Scott McAfee. Thanks also to the USDA, ARS, JPCS Natural Resource Conservation Center, Watkinsville, GA, for providing the soil used in the experiments.

REFERENCES

Cochrane, T.A., and D.C. Flanagan. 1996. Detachment in a simulated rill. Trans. ASAE 40:111–119.

Einstein, H., and N. Chien. 1955. Effects of heavy sediment concentration near the bed on velocity and sediment distribution. Rep. 8. Univ. of Calif., Berkley, Missouri River Div., U.S. Army Corps Eng.

Foster, G.R. 1982. Modeling the erosion process. p. 296–380. *In* C.T. Haan (ed.) Hydrologic modeling of small watersheds. ASAE, Joseph, MI.

Foster, G.R., L.J. Lane, J.D. Nowlin, J.M. Laflen, and R.A. Young. 1981. Estimating erosion and sediment yield on field-sized areas. Trans. ASAE 24:1253–1262.

Foster, G.R., and L.D. Meyer. 1972. A closed form soil erosion equation. p. 12.1–12.19. *In* H.W. Shen (ed.) Sedimentation (Einstein). Colorado State Univ., Fort Collins, CO.

Hairsine, P.B., and C.W. Rose. 1992a. Modeling water erosion due to overland flow using physical principles: 1. Sheet flow. Water Resour. Res. 28:237–244.

Hairsine, P.B., and C.W. Rose. 1992b. Modeling water erosion due to overland flow using physical principles: 2. Rill flow. Water Resour. Res. 28:245–250.

Huang, C., J.M. Bradford, and J.M. Laflen. 1996. Evaluation of detachment-transport coupling concept in the WEPP rill erosion equation. Soil Sci. Soc. Am. J. 60:734–739.

Lei, T., M.A. Nearing, K. Haghighi, and V.F. Bralts. 1998. Rill erosion and morphological evolution: A simulation model. Water Resour. Res. 34:3157–3168.

Li, G., A.D. Abrahams, and J.F. Atkinson. 1996. Correction factors in the determination of mean velocity of overland flow. Earth Surf. Processes Landforms 21:509–515.

Meyer, L.D., and E.J. Monke. 1965. Mechanics of soil erosion by rainfall and overland flow. Trans. ASAE 8:572–580.

Nearing, M.A. 1991. A probabilistic model of soil detachment by shallow turbulent flow. Trans. ASAE 34:81–85.

Nearing, M.A., G.R. Foster, L.J. Lane, and S.C. Finkner. 1989. A process-based soil erosion model for USDA-Water Erosion Prediction Project technology. Trans. ASAE 32:1587–1593.

Nearing, M.A., L.D. Norton, D.A. Bulgakov, G.A. Larionov, L.T. West, and K.M. Dontsova. 1997. Hydraulics and erosion in eroding rills. Water Resour. Res. 33:865–876.

Nearing, M.A., and S.C. Parker. 1994. Detachment of soil by flowing water under turbulent and laminar conditions. Soil Sci. Soc. Am. J. 58:1612–1614.

Nearing, M.A., S.C. Parker, J.M. Bradford, and W.E. Elliot. 1991. Tensile strength of 33 saturated unconsolidated soils. Soil Sci. Soc. Am. J. 55:1546–1551.

Raudkivi, A.J. 1990. Loose boundary hydraulics. Pergamon Press, Oxford.

Rice, C.T., and B.N. Wilson. 1990. Analysis of dynamic variables of rill flow. ASAE Paper 902011. ASAE, St. Joseph, MI.

Rose, C.W., K.J. Coughlan, and B. Fentie. 1998. Griffith University Erosion System Template (GUEST). p. 399–412. *In* J. Boardman and D.T. Favis-Mortlock (ed.) Modeling soil erosion by water. NATO-ASI Global Change Series. Springer-Verlag, Heidelberg.

Vanoni, V.A., and G.N. Nomicos. 1960. Resistance properties of sediment-laden streams. Trans. ASCE 125:1140–1175.

Wang, Z., and P. Larsen. 1994. Turbulent structure of water and clay suspension with bed load. J. Hydraulic Eng. 120:577–600.